



|              |   |
|--------------|---|
| Title        | Circular resonant cavities as basis of random lasing in $\pi$ -conjugated polymer films |
| Author(s)    | Palson, R. C.; Vardeny, Z. V.; Yoshino, Katsumi   |
| Citation     | 電気材料技術雑誌. 2011, 20(2), p. 71-77   |
| Version Type | VoR   |
| URL          | <a href="https://hdl.handle.net/11094/76881">https://hdl.handle.net/11094/76881</a>     |
| rights       |   |
| Note         |   |

*The University of Osaka Institutional Knowledge Archive : OUKA*

<https://ir.library.osaka-u.ac.jp/>

The University of Osaka

## Circular resonant cavities as basis of random lasing in $\pi$ -conjugated polymer films

R.C. Polson and Z.V. Vardeny

*Department of Physics and Astronomy, University of Utah, Salt Lake City Utah 84112 USA  
and*

K. Yoshino

Shimane Institute for Industrial Technology, 1 Hokuryo-cho, Matsue, Shimane 690-0816 Japan

### Abstract

Emission spectra from random lasing systems typically have numerous narrow emission lines. When excited very near laser threshold there are fewer emission lines and the emission lines are found to be highly correlated to one another. Fourier transform analysis of the emission spectrum shows circular resonant structures as the basis for the emission. We developed a mapping technique to spatially resolve the random laser emission from  $\pi$ -conjugated polymer films. By mapping the spatial locations from which the emission peaks originate, we unraveled bright areas that correspond to naturally formed resonant cavities. Mapping analysis at various excitation intensities shows multiple resonant microcavities that pass lasing threshold at different intensities.

### 1. INTRODUCTION

Systems which produce laser emission without an engineered cavity are grouped under the term *random lasers* (RL). Some of the many examples of RL include powders of laser crystals [1], dye and scatters in suspension [2] and solid forms, clusters of nanoparticles [3], films of  $\pi$ -conjugated polymers [4], liquid crystals and dye [5]. When the emission spectra from random lasing systems are presented, there are usually numerous sharp lines or peaks (>20) on top of a broader background of amplified spontaneous emission (ASE). Since there are so many peaks at high excitation intensities, subsequent analysis of the RL spectrum is complicated; and thus nearly any theoretical model that yields many laser lines can be used to model the resulting emission spectrum.

In contrast, in this work we look at RL spectra that are obtained just above lasing threshold. In particular we studied RL spectra near threshold excitation in  $\pi$ -conjugated polymer films. Under these conditions, since there are fewer resonant lines in the emission spectrum, it allows us to present a more credible analysis of the emission spectrum. Using Fourier transform analysis we found that the RL resonant lines are highly correlated to each other, and thus originate from a single resonant structure in the film. In support of this interpretation, we show that a novel mapping of the RL emission spectrum from the polymer films indeed unravels the existence of a number of naturally-formed microcavities having diverse threshold excitation intensities.

## 2. EXPERIMENTAL

Random lasing of  $\pi$ -conjugated polymer films has been well studied [6–8]. Here we investigate the RL emission modes of such system near threshold excitation intensity. The random lasing polymer film has both the gain medium and scatterers in the same material. The chain isomerization length of the polymer determines the solubility. By choosing a long chain isomerization length and poor solvent, the polymer powder may dissolve, but also form aggregates [9]. The aggregates act as scatterers and both the polymer film and aggregates play the role of the disordered gain medium. The specific polymer used here was poly (2,5-dihexyloxy-p-phenylenevinylene) (DHO-PPV) that we synthesized in house. The dry polymer powder was mixed in toluene and then heated until it was all dissolved. The solution was allowed to cool to 30° C and then spun cast onto a glass substrate to form neat films  $\sim 1 \mu\text{m}$  thick.

Optical excitation was provided from a Nd:YAG picosecond regenerative amplifier. The second harmonic at 532 nm was used at a repetition rate of 800 Hz. The measurements were performed in dynamic vacuum at pressure of  $\sim 100$  mT, since the polymer samples show photo-oxidation and signal degradation when excited in air. The excitation beam was focused onto a film of DHO-PPV using a spherical singlet lens. The emission from the excited film was collected with a 10x infinity corrected microscope objective. A third lens was used to couple light to a spectrograph; this lens was mounted on a computer controlled translation stage (a schematic diagram of the set-up is shown in figure 1). The emission light was dispersed with an imaging spectrograph, and the light was recorded with a two dimensional charge-coupled device (CCD) camera. The output of the CCD camera is wavelength and slit height. We note that each binned pixel from the CCD covers 9.6 microns in height and 0.02 nm in wavelength.

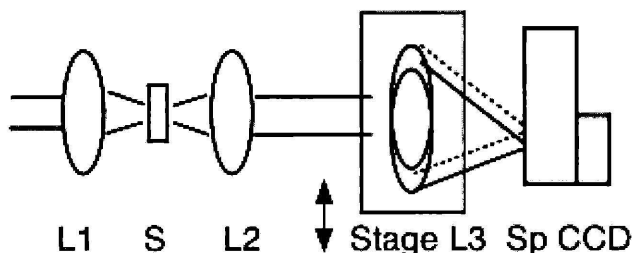


FIG. 1: Schematic of experimental set-up.

One of the characteristics properties of random lasing from polymers is that the spectrum changes when different area on the polymer film are excited. In order to probe the emission of the excited area, the excitation spot, sample, and microscope objective are all held fixed. Translating the third lens adjusts the segment of the excited area which is imaged. In this way, we could produce an emission map of the lasing film. This method has been used previously to show threshold dependence of RL in a polymer film [6], and was described in more detail in a later publication [10]. A different imaging method was used before, where the entire spectrum was recorded and an optical image was obtained [11].

## 3. RESULTS AND DISCUSSION

Figure 2(a) shows the collected emission spectrum from the polymer film just above RL threshold excitation. The RL emission spectrum has only a few sharp lines that are well-separated. Other random lasing systems have also shown very narrow and separated peaks in the emission spectrum [12]. The line spacing,  $\Delta\lambda$  is measured to be unequal; starting from the most intense peak,  $\Delta\lambda=0.55$  nm, then is reduced with  $\lambda$  to  $\Delta\lambda=0.51$  nm at the end of the gain spectrum. A linear cavity as a basis of the highly ordered RL emission spectrum here seems unlikely, since that cavity would give equally-spaced peaks. The very narrow and well-separated emission lines here should be able to be analyzed in some other way.

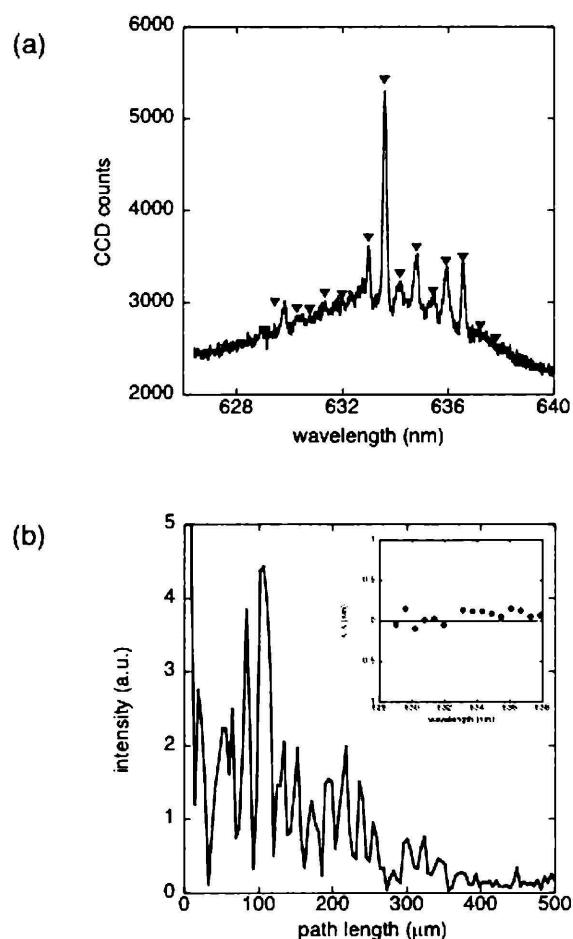


FIG. 2: (a) Random laser emission spectrum from a DHO-PPV polymer film. (b) Power Fourier transform of (a). Inset: difference between observed and calculated peak positions.

The tool we have employed to help analyze RL spectra is the power Fourier transform (PFT) of the emission spectrum [7]. Figure 2(b) presents the PFT of the emission in Fig. 2(a). The PFT shows very distinct peaks which indicate the presence of a resonant structure in the film. For a linear cavity the PFT peak spacing,  $\Delta d$  occurs at  $nL/\pi$ , where  $n$  is the index of refraction and  $L$  is the separation between the two mirrors. Since the peak spacing  $\Delta\lambda$  in the emission spectrum changes across the emission spectrum, then a linear cavity is not applicable, and thus some other resonant geometry may be more appropriate. The next highest dimensionality is two-dimensional (2D), and the simplest 2D structure is a circle. We try using the methods for

circular resonance cavities to analyze the spectrum in Fig. 2(a) [13]. In a 2D circular resonant structure, peaks in the PFT of the emission spectrum occur at  $\Delta d = nD/2$ , where  $n$  is the index of refraction and  $D$  is the diameter of the circle. Analysis of 2D circular resonant cavities leads to Bessel functions,  $J_m$ . The emission peaks in Fig. 2(a) are very narrow, which suggests a well- confined resonant cavity, because there is very little leakage from the resonant structure to the surroundings. In previous analysis of fabricated circular microstructures, an approximation was made that simplified the analysis [14]. The approximation is that the argument of the Bessel function goes to zero at the cavity boundary; i.e.  $J_m(\pi nD/\lambda) = 0$ , where  $m$  is the integer index of the Bessel function,  $n$  is the index of refraction, and  $D$  is the diameter. This 'zero condition' can be written as  $Z_{m,p} = \pi nD/\lambda$ , where  $p$  are indices of the zeros in the Bessel function  $m$ . Zeros of Bessel functions are numbers that can be calculated with various commercial software packages. With the product of  $nD$  obtained from the PFT spectrum, the predicted wavelengths can be readily calculated as following.

Our analysis starts with the most intense emission peak in Fig. 2 at 633.59 nm. The largest PFT peak provides a numerical value for the product  $nD = 106 \mu\text{m}$ . We first look at the first zero of high order Bessel functions, since this is the simplest configuration. Bessel function number 1061 has the first zero at 1080.03 and with  $nD$  of  $106 \mu\text{m}$ , this gives a calculated wavelength of 633.79 nm. Neighboring peaks in the RL emission spectrum correspond to successive Bessel functions. The emission peak at 636.55 nm, for example corresponds to  $J_{1056}$ ; whereas the emission peak at 629.8 nm corresponds to  $J_{1068}$ . In total there are 14 peaks in the RL emission spectrum near threshold that are assigned to 14 successive Bessel functions, all with the same value of  $nD$  which comes

directly from the Fourier transform. This procedure is more of an assignment rather than a fitting process, since there are no adjustable parameters. Some of the measured peaks are weak, and thus are difficult to distinguish from the noise. The inset of Fig. 2(b) shows the difference between the calculated and measured peak wavelengths.

Figure 2 and the analysis above indicate that the observed emission peaks are correlated to one another, and thus they result from the same underlying structure, regardless of the microcavity type used to analyze the RL spectrum in more details. But fitting a random lasing spectrum with a circular resonator seems surprising. However, there are actually several theoretical works which directly support this cavity type in a 2D disordered gain medium. A few works explicitly show that circular structures are likely formed for 2D random medium [15, 16]. Some calculated mode structures show modes at the boundary of a circular boundary [17]. There are works that discuss scattering in loops [18] [19]. There is another work that shows multiple narrow peaks from uncorrelated long scattering paths [20]. Another theoretical work describes emission from films that arise from small localized resonant structures [21].

To support our conclusion for circular microcavities in the film, the experimental set up shown in Fig. 1 allows an emission map to be created. By translating the third lens, different regions of the same area of the excited film may be probed. The film is photoexcited and the RL emission spectrum from a specific area on the film is recorded by a CCD camera. The lens is translated  $\sim 50$  microns which corresponds to 5 microns on the sample because of the 10x magnification inherent in the set-up. The process is repeated several times. The resulting data sets consist of CCD images in the form of wavelength versus height, repeated over stage position, namely  $f(\lambda, h, x)$ . Our first data set consists of

the polymer film excited just at lasing threshold of  $0.6 \mu\text{J/pulse}$ . All of the columns from the CCD image are summed in Fig. 3 to give an integrated wavelength intensity. Figure 3(a) shows the integrated emission spectrum at two film locations, namely  $35 \mu\text{m}$  and  $175 \mu\text{m}$ . Surprisingly the two RL emission spectra are very similar. The data set  $f(\lambda, h, x)$  allows some processing to further obtain information about the location of the RL emission in the film. The main peak in Fig. 3(a) is at  $633.5 \text{ nm}$ . It is possible to take the integrated intensity of this peak with a  $0.63 \text{ nm}$  wide window, and then calculate the intensity for each location of slit height and  $x$  position of the film,  $f(\Delta\lambda, h, x)$ . The resulting 2D image in false colored is shown in Fig. 3(b). The

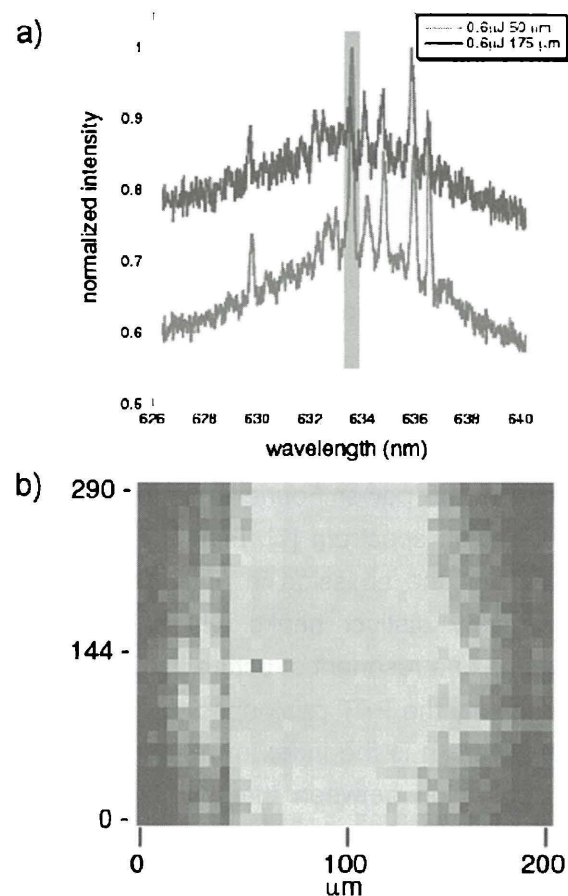


FIG. 3: (a) RL emission spectrum from positions  $50 \mu\text{m}$  and  $175 \mu\text{m}$  with excitation intensity  $1.2 \mu\text{J/pulse}$ . (b) Mapping intensity of the RL line shown in (a).



633.5 nm peak is most intense near  $x=55$  microns (row #10) in the middle; however it persists throughout most of the sample film.

The same film area was scanned at different excitation intensity. Figure 4(a) shows the emission spectra for the same two locations, of 5  $\mu\text{m}$  and 175  $\mu\text{m}$ . Figure 4(b) is the peak map at excitation intensity three times the threshold intensity, namely 1.7  $\mu\text{J}/\text{pulse}$ . The emission spectra are again very similar, but not the same (notice minor peaks near 630 nm). There are still narrow peaks, but there is a much stronger background coming from amplified spontaneous emission (ASE). The peak map shows a different picture than that at the lower intensity. In Fig. 4(b) the emission is strong in an area to the left in a

circular region. There is a second region on the right that also has stronger intensities.

The size of the bright region on the left is roughly 80  $\mu\text{m}$  wide and 220  $\mu\text{m}$  high. These numbers correspond rather well to the value of 212  $\mu\text{m}$  for a diameter of a circular cavity extracted from the Fourier transform in Fig. 2(b). The emission peaks can be described by circular Bessel functions, and in an independent determination the emission area is also roughly circular. We conclude that the circular area is in fact a naturally-formed microresonator within the random lasing medium. Earlier works utilized an average Fourier transform over many locations to try and extract a mean cavity size [7]. Total RL emission spectra over the entire emission area were used, and then the total spot translated. The present work shows the existence of a single resonator at threshold intensity, in agreement with the RL emission spectrum analysis using PFT.

We can now propose a framework to describe random lasing that incorporates many disparate facts. Near lasing threshold, laser emission starts from a single circular resonance structure. The emission peaks are not independent of one another, but are actually coming from the same circular resonant structure within the polymer film. The analysis of Fig. 2 as Bessel functions, and the emission map of Fig. 3 taken together demonstrate a circular structure. The emission radiates into the surrounding excited gain media. The surrounding gain media propagates and amplifies further the emission from the source resonant structure. The RL emission spectrum from the medium appears to be nearly the same across the photoexcited film spot even though it originates from a very localized region. At higher excitation intensities, as seen in Fig. 4(b), separate cavities cross lasing threshold and emit their own typical laser emission spectrum; but these cavities are still seeded by the first cavity with lower threshold. The resulting emission is a

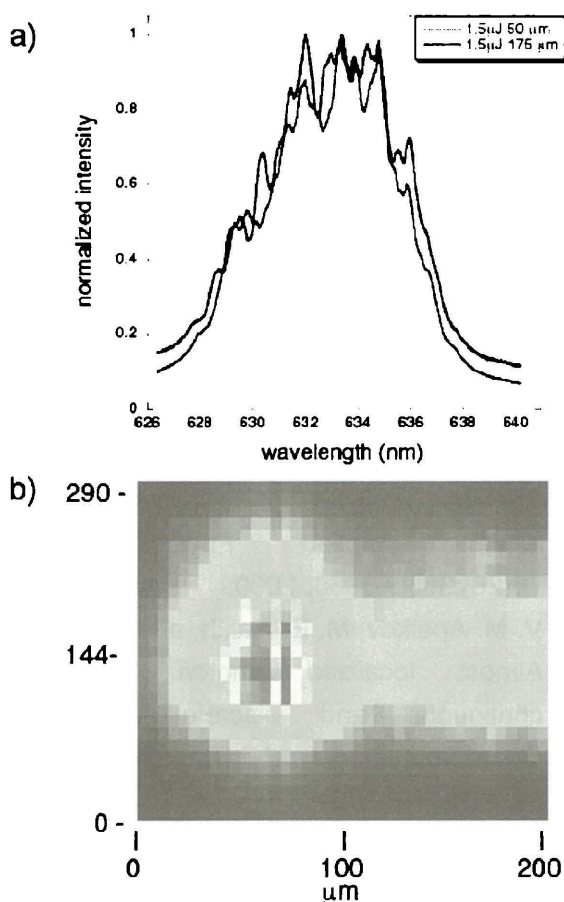


FIG. 4: (a) RL emission spectrum from positions 50  $\mu\text{m}$  and 175  $\mu\text{m}$  with excitation intensity 1.5  $\mu\text{J}/\text{pulse}$ . (b) Mapping intensity of the laser line shown in (a).

combination of the intrinsic cavity emission, the seeded emission, and the background ASE. We note that the lasing polymer film is only one example of random lasing. The same analysis likely applies to other random lasing systems especially when excited near lasing threshold [22].

We thank L. Wojchik for the polymer synthesis. This work was supported in part by the DOE under grant No. FG02-04ER46109.

- [1] C. Gouedard, D. Husson, C. Sauteret, F. Auzel, and A. Migus. Generation of spatially incoherent short pulses in laser-pumped neodymium stiochiometric crystals and powders. *J. Opt. Soc. Am. B.*, 10(12):2358–2363, 1993.
- [2] N.M. Lawandy, Balachandran R, M, A.S.L. Gomes, and E. Sauvain. Laser action in strongly scattering media. *Nature*, 368:436–438, 1994.
- [3] H. Cao, Y. G. Zhao, S. T. Ho, E. W. Seelig, Q. H. Wang, and R. P. H. Chang. Random laser action in semiconductor powder. *Phys. Rev. Lett.*, 82(11):2278–2281, Mar 1999.
- [4] S. V. Frolov, Z. V. Vardeny, K. Yoshino, A. Zakhidov, and R. H. Baughman. Stimulated emission in high-gain organic media. *Phys. Rev. B*, 59(8):R5284–R5287, Feb 1999.
- [5] G. Strangi, S. Ferjani, V. Barna, A. De Luca, C. Versace, N. Scaramuzza, and R. Bartolino. Random lasing and weak localization of light in dye-doped nematic liquid crystals. *Optics express*, 14(17):7737–7744, 2006.
- [6] A. Tulek, R. C. Polson, and Z. V. Vardeny. Threshold excitation statistics and imaging of random lasers in pi-conjugated polymer films; evidence for random resonators. *Nature Physics*, 6:303–310, 2010.
- [7] R.C. Polson, M.E. Raikh, and Z.V. Vardeny. Universal properties of random lasers. *Selected Topics in Quantum Electronics, IEEE Journal of*, 9(1):120–123, Jan-Feb 2003.
- [8] S.V. Frolov, M. Shkunov, A. Fujii, K. Yoshino, and Z. V. Vardeny. Lasing and stimulated emission in  $-\pi$  conjugated polymers. *Quantum Electronics, IEEE Journal of*, 36(1):2–11, 2000.
- [9] Thuc-Quen Nguyen, Vinh Doan, and Benjamin J. Schwartz. Conjugated polymer aggregates in solution: Control of interchain interactions. *Journal of Chemical Physics*, 110:4068–4078, 1999.
- [10] R.C. Polson and Z. V. Vardeny. Spatially mapping random lasing cavities. *Optics Letters*, 35(16):2801–2803, 2010.
- [11] Johannes Fallert, Roman J. B. Dietz, Janos Sartor, Daniel Schneider, and Claus Klingshirn Heinz Kalt. Co-existence of strongly and weakly localized random laser modes. *Nature Photonics*, 3:279–282, 2009.
- [12] Karen L. van der Molen, R. Willem Tjerkstra, Allard P. Mosk, and Ad Lagendijk. Spatial extent of random laser modes. *Physical Review Letters*, 98(14):143901, 2007.
- [13] R. C. Polson, Z. V. Vardeny, and D. A. Chinn. Multiple resonances in microdisk lasers of  $\pi$ -conjugated polymers. *Applied Physics Letters*, 81(9):1561–1563, 2002.
- [14] R. C. Polson, G. Levina, and Z. V. Vardeny. Spectral analysis of polymer microring lasers. *Applied Physics Letters* 76(26):3858–3860, 2000.
- [15] V. M. Apalkov, M. E. Raikh, and B. Shapiro. Almost localized photon modes in continuous and discrete models of disordered media. *J. Opt. Soc. Am. B* 21:132–140, 2004.
- [16] V. M. Apalkov, M. E. Raikh, and B. Shapiro. Random resonators and prelocalized modes in disordered dielectric films. *Phys. Rev. Lett.* 89(1):016802, Jun 2002.
- [17] H. E.Tureci, Li Ge, S. Rotter, and A. D. Stone. Strong interactions in multimode random lasers. *Science* 320(5876):643–646, 2003.

- 2008.
- [18] Regine Frank, Andreas Lubatsch, and Johann Kroha. Theory of strong localization effects of light in disordered loss or gain media. *Phys. Rev. B*, 73(24):245107, Jun 2006.
- [19] Meint P. van Albada, Bart A. van Tiggelen, Ad Lagendijk, and Adriaan Tip. Speed of propagation of classical waves in strongly scattering media. *Phys. Rev. Lett.*, 66(24): 3132–3135, Jun 1991.
- [20] S. Mujumdar, M. Ricci, R. Torre, and D. S. Wiersma. Amplified extended modes in random lasers. *Phys. Rev. Lett.*, 93(5):053903, Jul 2004.
- [21] R. Frank, A. Lubatsch, and J. Kroha. Light transport and localization in diffusive random lasers. *J. Opt. A: Pure & Appl. Opt.*, 11: 114012–114018, 2009.
- [22] R. Polson and Z. V. Vardeny. Random lasers at threshold excitation intensity. *Jour. of Synth. Metals* (in the press).